Journal of Alloys and Compounds 509 (2011) 9577–9582

Contents lists available at ScienceDirect

Journal of Alloys and Compounds

journal homepage: www.elsevier.com/locate/jallcom

First-principles study of the elastic and thermodynamic properties of HfB_2 with AlB_2 structure under high pressure

Ji-Dong Zhang[a,b,*], Xin-Lu Cheng[b], De-Hua Li[c]

[a] Department of Physics, School of Science, Shihezi University, Shihezi 832003, PR China
[b] Institute of Atomic and Molecular Physics, Sichuan University, Chengdu 610065, PR China
[c] College of Physics and Electronic Engineering, Sichuan Normal University, Chengdu 610066, PR China

ARTICLE INFO

Article history:
Received 19 April 2011
Received in revised form 22 July 2011
Accepted 25 July 2011
Available online 3 August 2011

Keywords:
HfB_2
First-principles calculation
Elastic and thermodynamic property
High pressure

ABSTRACT

Elastic and thermodynamic properties of HfB_2 with AlB_2 structure under pressure are investigated by means of density functional theory method. The results at zero pressure are in good agreement with available theoretical and experimental values. The pressure dependence of elastic constants, bulk modulus and elastic anisotropy of HfB_2 has been investigated. Through quasi-harmonic Debye model, the variations of the Debye temperature, heat capacity and thermal expansion with pressure and temperature are successfully obtained and discussed.

1. Introduction

Today, hard materials play an important role in modern industry. Although more and more new hard materials are synthesized, transition metal-diborides as a kind of hard materials still attract great attention due to their unique physical and chemical properties such as high hardness, high melting point and oxidation [1–7]. Hafnium diborides (HfB_2) is one of the transition metal-diborides with hexagonal AlB_2 structure, which can be applied to thin film resistors [8] and explored as diffusion barriers in microelectronics [9,10]. Because of these properties, HfB_2 has been widely investigated in literatures. Chen et al. [11] and Sonber et al. [12] reported the synthesis of HfB_2 in different methods. Shein and Ivanovskii [13] studied the structural and elastic properties of HfB_2 using first-principles calculations. Vajeeston et al. [14] calculated the electronic structure, bonding and ground state properties. Also Zhang et al. [15] investigated the electronic structure, bonding, as well as hardness, and reported that HfB_2 is of metallicity. Kaur et al. [16] studied the cohesive and thermal properties. Deligoz et al. [17] studied the phonon dispersion and thermodynamic property. Hao et al. [18] investigated the trends in elasticity and electronic structure of 5d transition metal-diborides in the *Pmmn* space group.

For a hard material, a detailed investigation under high pressure is necessary because pressure can effectively tune physical properties of material. Electronic, elastic and thermodynamic properties of a solid under pressure are closely related to compressibility, hardness, transport properties and other characteristics. Moreover, we also can directly obtain some useful information on the characteristics of a crystal. However, to the best of our knowledge, the pressure effect on the properties of HfB_2 has rarely been reported except for our recent study on pressure-induced electronic behaviors [19]. In this paper, we focus our attention on the elastic and thermodynamic properties of HfB_2 with AlB_2 structure under high pressures. For this purpose, we investigate and discuss elastic constants, Debye temperature and some other thermodynamic properties such as heat capacity and thermal expansion coefficient for HfB_2 at different pressures using density functional theory calculations, which have been widely employed to calculate properties of materials as a supplement to experiment.

2. Model and computational method

HfB_2 crystallizes in hexagonal AlB_2 structure with a space group P6/mmm (No. 191). There are three atoms in a unit cell, in which Hafnium atom occupies the origin and two Boron atoms hold the 2d Wychoff site (1/3, 2/3, 1/2). In present calculations, the initial lattice parameters $a = 3.141$ Å, $c = 3.470$ Å are from experiment [20]. Calculations are performed based on the plane-wave pseudopotential density-functional theory (DFT) [21,22] as implement in CASTEP Package [23]. We employ Vanderbilt ultrasoft pseudopotentials [24] to describe the electron-ion interactions in the calculation. Pseudoatomic calculations are performed for Hf $5d^2 6s^2$ and B $2s^2 2p^1$. The exchange correlation energy is described in the generalized gradient approximation (GGA) using the Perdew–Burke–Ernzerhof (PBE) functional [25]. Crystal

* Corresponding author at: Department of Physics, School of Science, Shihezi University, Shihezi 832003, PR China.
E-mail address: lzzjd@126.com (J.-D. Zhang).

0925-8388/$ – see front matter © 2011 Elsevier B.V. All rights reserved.
doi:10.1016/j.jallcom.2011.07.093

Table 1
The calculated structural data of HfB_2 under zero pressure and related experimental and theoretical data.

Structure	Present work	[a]Experiment	Other work
a (Å)	3.165	3.141	3.144[b] 3.166[c] 3.131[d] 3.127[e]
c (Å)	3.511	3.470	3.502[b] 3.499[c] 3.409[d] 3.403[e]
c/a	1.109	1.105	1.114[b] 1.105[c] 1.089[d] 1.089[e]
Hf-B (Å)	2.534	2.510	2.530[c] 2.484[d] 2.481[e]
B-B (Å)	1.827	1.813	1.828[c] 1.807[d] 1.806[e]
B_0 (GPa)	260.9	–	270[b] 216[c] 256[e]
B_0'	4.16	–	3.68[e]

[a] Ref. [20], experiment.
[b] Ref. [13], GGA.
[c] Ref. [14], LDA.
[d] Ref. [17], GGA.
[e] Ref. [19], GGA.

structure is optimized with the Broyden–Fletcher–Goldfarb–Shanno (BFGS) [26] method. In calculations, plane-wave basis sets with energy cut-off 360.0 eV and $9 \times 9 \times 8$ Monkhorst–Pack mesh are used, while the self-consistent convergence of the total energy is 5×10^{-6} eV/atom, the maximum force on the atom below 10^{-2} eV/Å, and all the stress components less than 0.02 GPa. All parameters have been tested for convergence. During the structure optimizations, the total energy is minimized by varying lattice constants and internal atomic positions under the restriction of the given symmetry. Furthermore, the quasi-harmonic Debye model [27], which is constructed from the Helmholtz free energy at the temperature below the melting point in the quasi-harmonic approximation, is applied to obtain thermodynamic properties of HfB_2.

3. Results and discussion

3.1. Structure properties

Both lattice and internal coordinates of the HfB_2 compound have been fully optimized under several pressures using BFGS method [26]. The obtained cell volumes and corresponding pressures are fitted to the Birch–Murnaghan equation of state to get the bulk modulus (B_0) and its pressure derivative (B_0') under zero pressure. Table 1 lists the calculated equilibrium lattice constants, bond lengths, bulk modulus (B_0), and the pressure derivative of the bulk modulus (B_0'), together with the available experimental data and others' works. We find that the calculated results are in good agreement with the experimental [20] and previous theoretical values [13,14,17,19]. The satisfying performance makes us feel confident in further investigating properties of HfB_2 under high pressures.

The pressure dependence of ratios a/a_0, c/c_0, c/a, and normalized volume v (V/V_0) are obtained and shown in Fig. 1, where a_0, c_0 and V_0 are the zero pressure equilibrium structural parameters, respectively. As Fig. 1 shows, all ratios we plotted decrease smoothly with pressure. The crystal cell along c-axis is slightly more compressible than that along a-axis. When the applied pressure is up to 100 GPa, they are shortened only about 8.3% and 7.1%, respectively. Correspondingly, the volume of primitive cell decreases about 20.9% at 100 GPa. The ratio c/a exhibits a small change ranging from 1.109 at 0 GPa to 1.096 at 100 GPa, with a decrease about only 1.17%. It is clear that those values (a/a_0, c/c_0, c/a and V/V_0) all change in a quadratic manner with pressure. We make a fitting and obtain the following relationships:

$$\frac{a}{a_0} = 0.99909 - 0.00101p + 3.1327 \times 10^{-6}p^2 \quad (1)$$

$$\frac{c}{c_0} = 0.99863 - 0.00124p + 4.3858 \times 10^{-6}p^2 \quad (2)$$

$$\frac{c}{a} = 1.10904 - 0.00026p + 1.3718 \times 10^{-6}p^2 \quad (3)$$

$$\frac{V}{V_0} = 0.99631 - 0.00317p + 1 \times 10^{-5}p^2 \quad (4)$$

Moreover, the calculations show that the volume compressibility [$\mathrm{d}(\ln V)/\mathrm{d}p = -0.0033\ \mathrm{GPa}^{-1}$] of HfB_2, obviously lower than the values of MgB_2 ($-0.0076\ \mathrm{GPa}^{-1}$) [28] and AlB_2 ($-0.0050\ \mathrm{GPa}^{-1}$) [29], is close to that of ReB_2 ($-0.00251\ \mathrm{GPa}^{-1}$) [30] which is taken as a low-compressible material [30]. The interlayer linear compressibility [$\mathrm{d}(\ln c)/\mathrm{d}p = -0.00126\ \mathrm{GPa}^{-1}$] is about 1.24 times larger than that in the basal plane [$\mathrm{d}(\ln a)/\mathrm{d}p = -0.00102\ \mathrm{GPa}^{-1}$], which also suggests that c axis is more compressible than a axis.

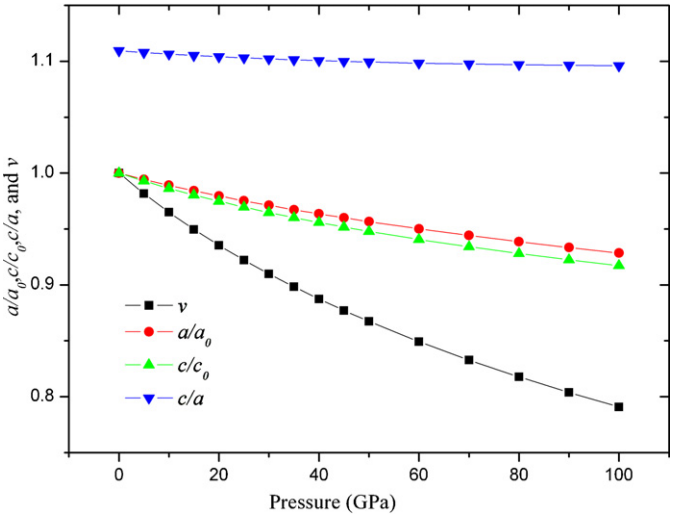

Fig. 1. Variation of ratios a/a_0, c/c_0, c/a and v as a function of pressure.

3.2. Elastic properties

Elastic property, an important property of solid, is closely related to various fundamental physical properties, such as specific heat, melting point, Debye temperature, thermal expansion coefficient, and so on. Now, we turn to study the elastic properties of HfB_2. The five independent elastic constants of HfB_2 (hexagonal crystal) are successfully obtained and listed in Table 2, as well as the calculated bulk modulus B, shear modulus G, Young's modulus E, Poisson's ratio v, and B/G at 0 GPa.

Also shown in Table 2 are B_a and B_c used to represent the mechanical anisotropy, which can be computed using the bulk moduli along the a and c axes respectively, and defined as follows [31]:

$$B_a = a\frac{dp}{da} = \frac{\Lambda}{2+\alpha}, \quad (9)$$

$$B_c = c\frac{dp}{dc} = \frac{B_a}{\alpha}, \quad (10)$$

$$\Lambda = 2(C_{11}+C_{12}) + 4C_{13}\alpha + C_{33}\alpha^2, \quad (11)$$

$$\alpha = \frac{C_{11}+C_{12}-2C_{13}}{C_{33}-C_{13}}. \quad (12)$$

Table 2
Calculated elastic constants C_{ij} (GPa), the bulk moduli B_a and B_c (GPa), bulk modulus B (in GPa), shear modulus G (GPa), Young's modulus E (GPa), Poisson's ratio ν, and B/G at 0 GPa in comparison with available data.

	C_{11}	C_{12}	C_{13}	C_{33}	C_{44}	B_a	B_c	B	G	E	ν	B/G
Our work	583.3	98.4	131.8	456.2	257.7	851	661	260	233	538	0.155	1.12
Other work[a]	592.7	99.6	141.3	481.3	262.3	–	–	270	240	558	0.166	1.17

[a] Ref. [13], GGA.

It is obvious that the calculated elastic constants are in accordance with the data of Shein and Ivanovskii [13], while bulk modulus B, shear modulus G and Young's modulus E have relatively large deviation (about 4%) which may origin from different code employed in calculation. This suggests our calculations for elastic properties are reliable. The calculated small ratio B_a/B_c (1.287) is smaller than that of MgB_2 (2.10) [28] and TiB_2 (1.54) [32], indicating the stronger chemical bonding for HfB_2. Since the large value of Young's modulus (538 GPa), it will be stiff [33]. In addition, the low value of the B/G (less than 1.75) suggests that it is brittle [33,34]. In addition, our results satisfy the well-known Born stability criteria [35] ($C_{12} > 0$, $C_{33} > 0$, $C_{66} = (C_{11} - C_{12})/2 > 0$, and $(C_{11} + C_{12})C_{33} - 2C_{13}^2 > 0$) despite the applied pressure is up to 100 GPa, which shows that HfB_2 is mechanically stable. To further illustrate the effect of pressure on the elastic properties of HfB_2, we exhibit the variations of elastic constants, the bulk moduli B, bulk moduli B_a, B_c and the ratio B_a/B_c with pressure in Figs. 2 and 3, respectively. As Fig. 2 shows, the five independent elastic constants and bulk modulus increase monotonically with pressure. C_{11} and C_{33} vary rapidly under the effect of pressure in comparison with the variations in C_{12}, C_{13} and C_{44}, which is the same as the cases of ZrB_2 [36] and NbB_2 [37]. Furthermore, we have also fitted the variations of five constants as well as the bulk modulus to the following relationships:

$$C_{11} = 585.9 + 6.584p - 0.00846p^2, \quad (13)$$

$$C_{12} = 98.4 + 2.185p - 0.00031p^2, \quad (14)$$

$$C_{13} = 135.1 + 3.110p - 0.00003p^2, \quad (15)$$

$$C_{33} = 461.0 + 5.941p - 0.0064p^2, \quad (16)$$

$$C_{44} = 258.6 + 3.109p - 0.00476p^2, \quad (17)$$

$$B = 262.5 + 4.002p - 0.00268p^2; \quad (18)$$

From above relationships, we expect to obtain elastic constants and bulk modulus under even more high pressures. In addition, since the quadratic terms in these relationships make very limited contributions to total values, it seems like linear dependence of pressure for the elastic constants and bulk modulus. Fig. 3 shows the variations of normalized B_a, B_c and ratio B_a/B_c. As Fig. 3 shows, B_a and B_c increase with applied pressure, while the ratio B_a/B_c decreases with pressure. It is demonstrated that the anisotropy will weaken with increasing pressure.

At low temperatures, the Debye temperature, an important physical quantity of solid, can be calculated from elastic constants. We have calculated the Debye temperature, Θ_D, from elastic constants using the average sound velocity v_m, via the following relations [38]:

$$\Theta_D = \frac{h}{k}\left[\frac{3n}{4\pi}\left(\frac{N_A\rho}{M}\right)\right]^{1/3} v_m, \quad (19)$$

Here h is Planck's constants, k the Boltzmann's constant, N_A the Avogadro's number, n the number of atoms per formula unit, M the molecular mass per formula unit, and ρ the density. The average wave velocity v_m can be obtained from

$$v_m = \left[\frac{1}{3}\left(\frac{2}{v_s^3} + \frac{1}{v_p^3}\right)\right]^{-1/3}, \quad (20)$$

Here v_p and v_s are the compressional and shear wave velocity, respectively. They can be calculated from the Navier's equation [39]:

$$v_p = \sqrt{\frac{B + (4/3)G}{\rho}}, \quad \text{and} \quad v_s = \sqrt{\frac{G}{\rho}}; \quad (21)$$

Here B and G are the bulk and shear modulus, respectively. The calculated Debye temperature of HfB_2 at 0 GPa and 0 K condition is 698.4 K, which is close to those of MgB_2 (819 K) [40] and NbB_2 (862.9 K) [37]. The pressure effect on the Debye temperature of HfB_2 is also obtained and plotted in Fig. 4. Fig. 4 shows that the Debye temperature increases monotonically with pressure.

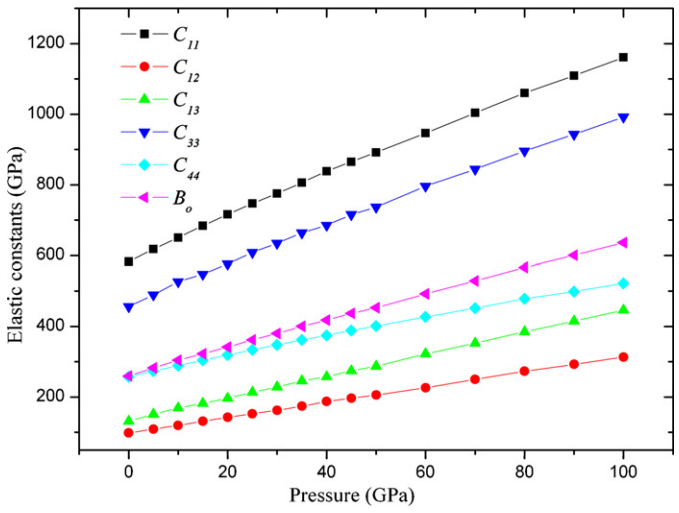

Fig. 2. Variation of elastic constants and bulk modulus as a function of pressure.

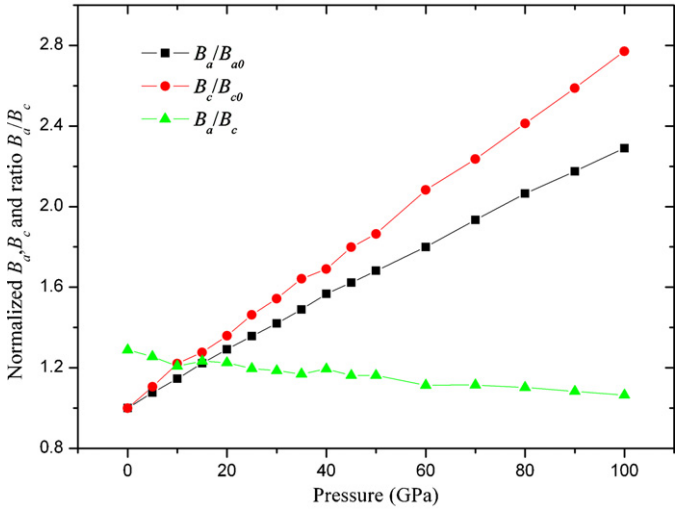

Fig. 3. Variation of B_a, B_c and the ratio B_a/B_c with increasing pressure.

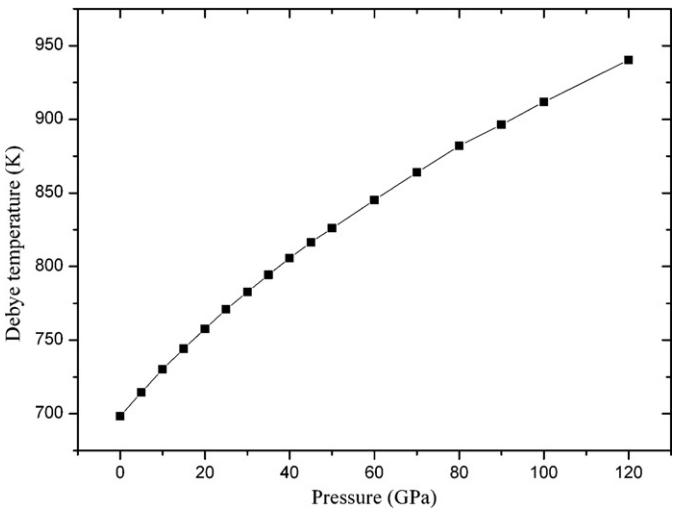

Fig. 4. Variation of Debye temperature with increasing pressure.

3.3. Thermodynamic properties

In order to systematically investigate thermodynamic properties of HfB_2, the quasi-harmonic Debye model [27] is introduced. Blanco et al. presented a simple methods to investigate thermodynamic properties of solid. Based on the equation of state and quasi-harmonic Debye model, the Debye temperature can be generated. Then we can obtain the non-equilibrium Gibbs function $G^*(V; P, T)$ from:

$$G*(V;P,T) = E(V) + PV + A_{Vib}(\Theta(V);T) \tag{22}$$

Here $E(V)$ is the total energy per unit cell for HfB_2, $\Theta(V)$ is the Debye temperature, and A_{Vib} represents vibrational Helmholtz free energy. Since the rigorous statistical calculation of A_{Vib} requires knowledge of the exact vibrational levels, it is customary to introduce the quasi-harmonic approximation:

$$A_{Vib}(\Theta;T) = nkT\left[\frac{9}{8}\frac{\Theta}{T} + 3\ \ln(1-e^{-\Theta/T}) - D\left(\frac{\Theta}{T}\right)\right] \tag{23}$$

Here $D(\Theta/T)$ represents the Debye integral, and n is the number of atoms per formula unit. For an isotropic solid,

$$\Theta = \frac{\hbar}{K}[6\pi^2 V^{1/2} n]^{1/3} f(\sigma)\sqrt{\frac{B_s}{M}}, \tag{24}$$

Here K is the Boltzman constant, M the molecular mass per formula unit, B_s the adiabatic bulk modulus. The Poisson ratio σ is computed as in Ref. [41]

$$\sigma = \frac{1}{2}\left[\frac{B-(2/3)G}{B+(1/3)G}\right] \tag{25}$$

And is taken as 0.1546. According to Ref. [42,43], $f(\sigma)$ equals to 1.040966. The non-equilibrium Gibbs function $G^*(V; P, T)$ can be minimized with respect to volume V as follows:

$$\left(\frac{\partial G*(V;P,T)}{\partial V}\right)_{P,T} = 0, \tag{26}$$

By solving above equation, one can obtain the thermal equation-of-state (EOS) $V(P, T)$. The isothermal bulk modulus and other thermal properties such as heat capacity at constant volume C_V, the heat capacity at constant pressure C_P, and thermal expansion α, respectively, are taken as

$$B_T(P,T) = -V\left(\frac{\partial P}{\partial V}\right) = V\left(\frac{\partial^2 G*(V;P,T)}{\partial V^2}\right)_{P,T}, \tag{27}$$

$$C_V = 3nk\left[4D\left(\frac{\Theta}{T}\right) - \frac{3\Theta/T}{e^{\Theta/T}-1}\right], \tag{28}$$

$$\alpha = \frac{\gamma C_V}{B_T V}, \tag{29}$$

$$C_P = C_V(1+\alpha\gamma T). \tag{30}$$

where γ is the Grüneisen parameter, and

$$\gamma = -\frac{d\ \ln\Theta(V)}{d\ \ln V}, \tag{31}$$

In Fig. 5, we present the obtained pressure-dependence (a) and temperature-dependence (b) of Debye temperature. The Debye temperature at 0 K and 0 GPa calculated using quasi-harmonic Debye model is 689.3 K, which is in good agreement with our above result (698.4 K) derived from elastic constants. This suggests our results about elastic and thermodynamic properties of HfB_2 are reliable. We observe from Fig. 5 that at a given temperature, the Debye temperature Θ increases with pressure; while it decreases with temperature when the pressure keeps constant. The effect of the temperature on the Debye temperature Θ is obviously smaller than that of the pressure. Especially, the temperature exhibits very limited effect on the Debye temperature Θ at high pressure, i.e. at 90 GPa, Θ decreasing only 2.33% when the temperature increases from 0 K to 1500 K. In addition, the Debye temperatures Θ at 1200 K are lower than those at 300 K, indicating that the vibration frequency of the particles in HfB_2 changes with the pressures and the temperatures [44].

The variations of heat capacity at constant volume C_V with pressure and temperature are depicted in Fig. 6a and b, respectively. Different with the Debye temperature Θ, C_V increases with temperature but decreases with pressure. It is clear that C_V is more sensitive to the temperature than to the pressure. In addition, Fig. 6a shows that the effect of the pressure on C_V gradually decreases with increasing temperature. From Fig. 6b, we find there are general features of the C_V, which are in good agreement with other study [17]. As Fig. 6b shows, when the pressure keeps constant, C_V increases rapidly when the temperature increases from 0 K to 400 K; when $T > 400$ K, C_V increases slowly with the temperature and almost approaches to a constant (Dulong–Petit limit) at higher temperatures, i.e. the calculated C_V at 0 GPa and 1500 K (74.2 J mol^{-1} K^{-1}) is close to Dulong–Petit limit $9N_Ak_B$ (74. 8 J mol^{-1} K^{-1}), where N_A is the Avogadro's number, and k_B is the Boltzmann's constant. In addition, the calculated C_V at 0 GPa and 1000 K is 73.2 J mol^{-1} K^{-1} ($8.8\,N_Ak_B$), which is in agreement with the value of $8.6\,N_Ak_B$ presented by Deligoz et al. [17].

The dependences of the thermal expansion α with the pressure and temperature are shown in Fig. 7a and b, respectively. As shown in Fig. 7a, the thermal expansion α decreases with pressure; the higher the temperature is, the faster the thermal expansion α decreases with pressure; and furthermore, the decrease becomes slower as pressure increases. Fig. 7b shows the thermal expansion α increases with temperature; it increases with T^3 at low temperatures, and approaches to a linear increase when $T > 600$ K, and the propensity of increment becomes moderate, which indicates that the temperature dependence of α is small at high temperature; in addition, the lower the pressure is, the greater the effect of temperature on the thermal expansion α is.

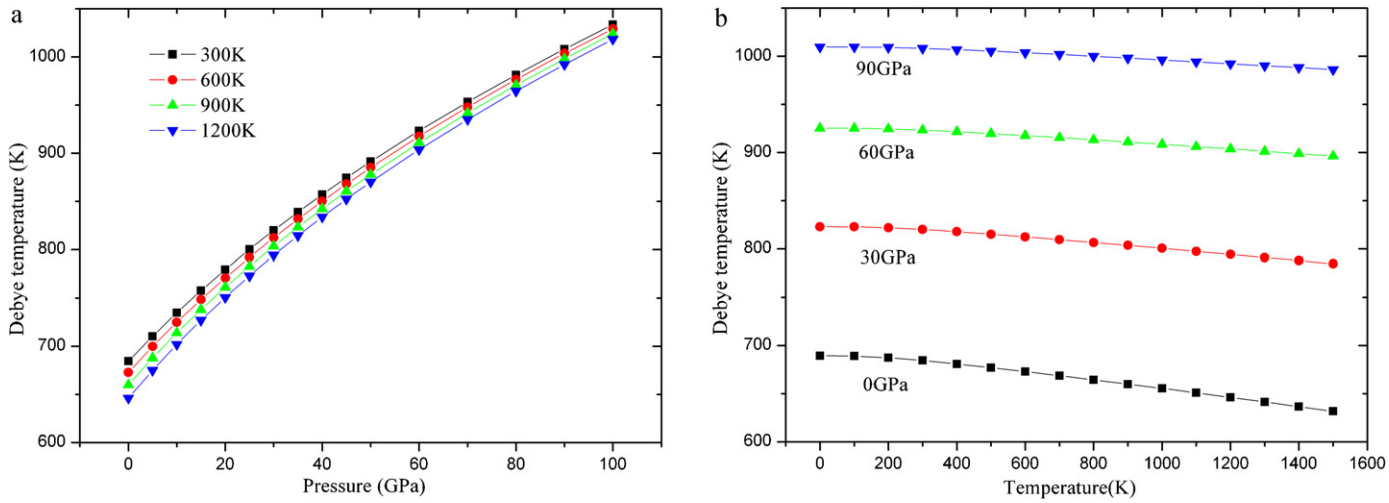

Fig. 5. The pressure (a) and temperature (b) dependence of Debye temperature calculated using quasi-harmonic Debye model.

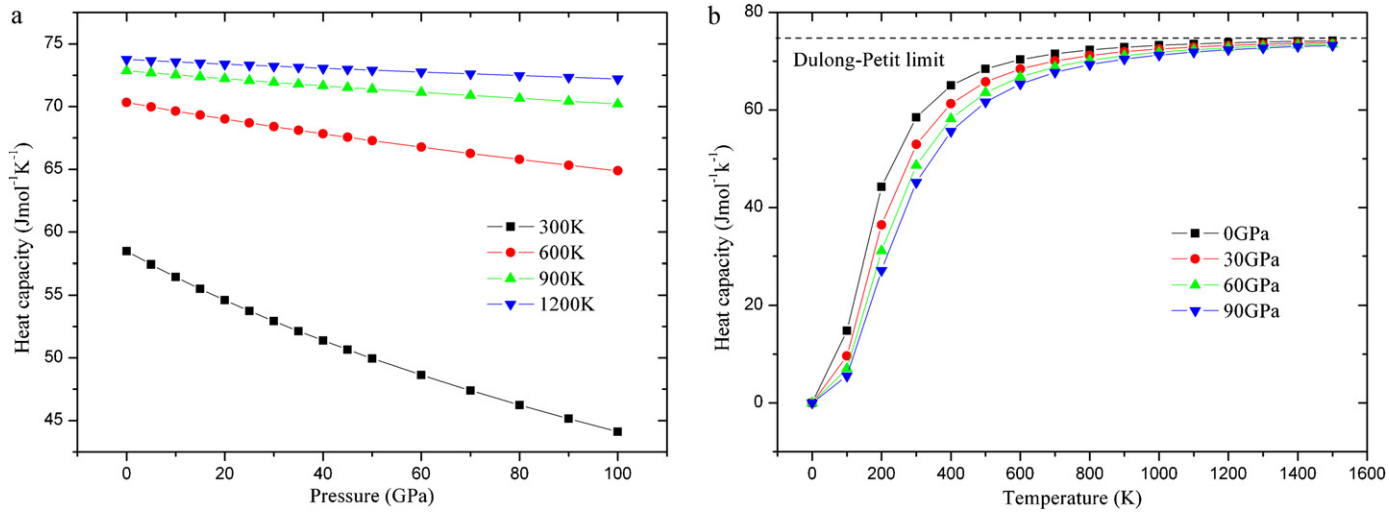

Fig. 6. The pressure (a) and temperature (b) dependence of heat capacity C_V.

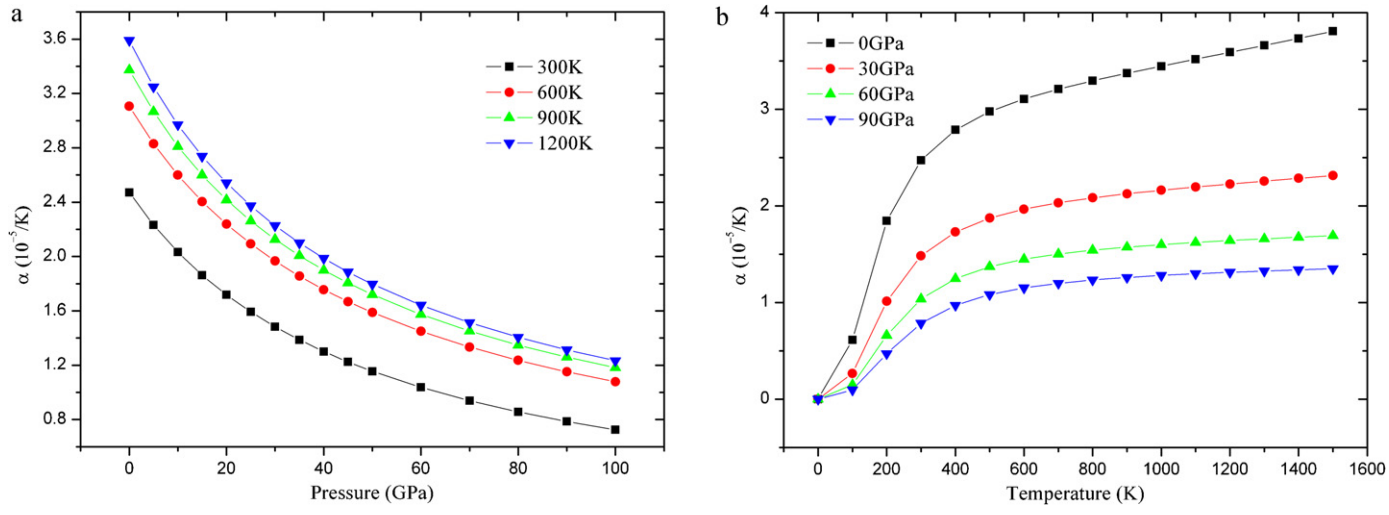

Fig. 7. The pressure (a) and temperature (b) dependence of thermal expansion α.

4. Conclusions

In this paper, we have investigated the elastic and thermodynamic properties of HfB_2 with AlB_2 structure using density functional theory within the generalized gradient approximation (GGA). The obtained lattice parameters, equilibrium volume, bulk modulus at ambient pressure are in good agreement with the experimental and theoretical values. The elastic constants and bulk modulus exhibit a nearly linear increase with pressure. Through the quasi-harmonic Debye model, the pressure and temperature dependence of Debye temperature, heat capacity and thermal expansion are obtained. It is found that the Debye temperature increases with pressure and decreases with temperature, which is contrary to the changes of the heat capacity and thermal expansion with pressure and temperature.

References

[1] R.A. Varin, C. Chiu, S. Li, D. Wexler, J. Alloys Compd. 370 (2004) 230.
[2] L.A. Shi, Y. Gu, L.Y. Chen, Z.H. Yang, Y.T. Qian, Mater. Lett. 58 (2004) 23.
[3] A. Erdemir, M. Halter, G.R. Fenske, Wear 205 (1997) 236.
[4] J. Nagamatsu, N. Nakagawa, T. Muranaka, Y. Zenitani, J. Akimitsu, Nature 410 (2001) 63.
[5] I.R. Shein, A.L. Ivanovskii, Phys. Rev. B 73 (2006) 144108.
[6] W. Zhou, H. Wu, T. Yildirim, Phys. Rev. B 76 (2007) 184113.
[7] C. Mitterer, J. Solid State Chem. 133 (1997) 279.
[8] D.S. Wuu, M.L. Lee, T.Y. Lin, R.H. Horng, Mater. Chem. Phys. 45 (1996) 163.
[9] C.S. Choi, G.A. Ruggles, A.S. Shah, J.D. Hunn, J. Electrochem. Soc. 138 (1991) 3062.
[10] G. Sade, J. Pelleg, Appl. Surf. Sci. 91 (1995) 263.
[11] L.Y. Chen, Y.L. Gu, Y.T. Qian, J. Alloys Compd. 368 (2004) 353.
[12] J.K. Sonber, T.S.R.Ch. Murthy, A.K. Suri, Int. J. Refract. Met. Hard Mater. 28 (2010) 201.
[13] I.R. Shein, A.L. Ivanovskii, J. Phys.: Condens. Matter 20 (2008) 415218.
[14] P. Vajeeston, P. Ravindran, C. Ravi, R. Asokamani, Phys. Rev. B 63 (2001) 045115.
[15] X.H. Zhang, X.G. Luo, W.B. Han, Comput. Mater. Sci. 44 (2008) 411.
[16] N. Kaur, R. Mohan, R.K. Singh, Physica B 404 (2009) 1607.
[17] E. Deligoz, K. Colakoglu, Y.O. Ciftci, Comput. Mater. Sci. 47 (2010) 875.
[18] X.F. Hao, Z.J. Wu, J. Meng, J. Phys.: Condens. Matter 19 (2007) 196212.
[19] J.D. Zhang, X.L. Cheng, Physica B 405 (2010) 3532.
[20] P. Villars, Pearson's, Handbook: Crystallographic Data for Intermetallic Phases, ASM International, Materials Park, OH, 1997.
[21] P. Hohenberg, W. Kohn, Phys. Rev. B 136 (1964) 864.
[22] W. Kohn, L.J. Sham, Phys. Rev. A 140 (1965) 1133.
[23] V. Milman, B. Winkler, J.A. White, C.J. Packard, M.C. Payne, E.V. Akhmatskaya, R.H. Nobes, Int. J. Quantum Chem. 77 (2000) 895.
[24] D. Vanderbilt, Phys. Rev. B 41 (1990) 7892.
[25] J.P. Perdew, K. Burke, M. Ernzerhof, Phys. Rev. Lett. 77 (1996) 3865.
[26] T.H. Fischer, J. Almlof, J. Phys. Chem. 96 (1992) 9768.
[27] M.A. Blanco, E. Francisco, V. Luana, Comput. Phys. Commun. 158 (2004) 57.
[28] H.Y. Wang, X.R. Chen, W.J. Zhu, Y. Cheng, Phys. Rev. B 72 (2005) 172502.
[29] K. Liu, X.L. Zhou, X.R. Chen, W.J. Zhou, Physica B 388 (2007) 213.
[30] X.L. Zhu, D.H. Li, X.L. Cheng, Solid State Commun. 147 (2008) 301.
[31] P. Ravindran, P. Vajeeston, R. Vidya, A. Kjekshus, H. Fjellvag, Phys. Rev. B 64 (2001) 224509.
[32] P.S. Spoor, J.D. Maynard, M.J. Pan, D.J. Green, J.R. Hellmann, T. Tanaka, Appl. Phys. Lett. 70 (1997) 1959.
[33] E. Deligoz, K. Colakoglu, Y.O. Ciftci, J. Mater. Sci. 45 (2010) 3720.
[34] S.F. Pugh, Philos. Mag. 45 (1954) 833.
[35] M. Born, Proc. Cambridge Philos. Soc. 36 (1940) 160.
[36] H.Z. Fu, Y. Lu, W.F. Liu, T. Gao, J. Mater. Sci. 44 (2009) 5618.
[37] X.F. Li, G.F. Ji, F. Zhao, X.R. Chen, D. Alfe, J. Phys.: Condens. Matter 21 (2009) 025505.
[38] O.L. Anderson, J. Phys. Chem. Solids 24 (1963) 909.
[39] E. Screiber, O.L. Anderson, N. Soga, Elastic Constants and their Measurements, McGraw-Hill, New York, 1973.
[40] T. Ichitsubo, H. Ogi, S. Nishimura, T. Seto, M. Hirao, H. Inui, Phys. Rev. B 66 (2002) 052514.
[41] B. Mayer, H. Anton, E. Bott, M. Methfessel, J. Sticht, P.C. Schmidt, Intermetallics 23 (2003).
[42] E. Francisco, J.M. Recio, M.A. Blanco, A. Martín Pendás, J. Phys. Chem. 102 (1998) 1595.
[43] E. Francisco, G. Sanjurjo, M.A. Blanco, Phys. Rev. B 63 (2001) 094107.
[44] H.Z. Fu, M. Teng, T. Gao, Physica B 405 (2010) 846.